Catalysis Communications 46 (2014) 146–149

Contents lists available at ScienceDirect

Catalysis Communications

journal homepage: www.elsevier.com/locate/catcom

Short Communication

One-pot synthesis of PdBi/reduced graphene oxide catalyst under microwave irradiation used for formic acid electrooxidation

Ruiqin Liu, Feifei Liu, Dongying Fu, Yunfei Bai, Gaoyi Han *, Yanni Tian *, Miaoyu Li, Yaoming Xiao, Yanping Li

Institute of Molecular Science, Shanxi University, Taiyuan 030006, PR China

ARTICLE INFO

Article history:
Received 13 October 2013
Received in revised form 6 December 2013
Accepted 9 December 2013
Available online 18 December 2013

Keywords:
Graphene
Pd
PdBi
Nanocomposites
Electrooxidation
Energy storage and conversion

ABSTRACT

The Pd and PdBi nanoparticles dispersed on the reduced graphene oxide (Pd/rGO and PdBi/rGO) have been synthesized through one-pot reaction under the irradiation of microwave and the obtained composites have been characterized by transmission electron microscopy, X-ray diffraction and X-ray photoelectron spectroscopy, and their electrocatalytic activities have also been evaluated. It is found that the $PdBi_{0.05}$/rGO catalyst exhibits higher activity and better stability toward formic acid electrooxidation compared with Pd/C and Pd/rGO. The excellent electrocatalytic performance indicates that the addition of appropriate amount of Bi can greatly enhance the activity and stability of Pd catalysts for the formic acid oxidation.

1. Introduction

Compared with methanol, formic acid is less toxic, less flammable and has much lower fuel crossover and faster oxidation kinetics. Furthermore, the power density of the direct formic acid fuel cell (DFAFC) is much higher than that of direct methanol fuel cell (DMFC) although its energy density is lower than that of DMFC [1–4]. Therefore, DFAFC has attracted increasing attention and been considered to be an attractive candidate for mobile and portable power devices [5–7].

To increase the electrocatalytic activity and reduce the noble metal loading, much effort has been made to develop highly dispersed metal nanoparticles (NPs) on the supports including activated carbon, carbon nanotubes [8], carbon nanofibers [9] and graphene [10]. Most investigations have demonstrated that Pd nanoparticles show much higher activity for formic acid oxidation than Pt catalysts [7,11]. However, the stability of Pd/C catalysts must be further improved due to the aggregation of Pd particles and the accumulation of CO-like intermediates on Pd particles during the electrooxidation process of formic acid [5,6]. It has been proved that the addition of the second element can effectively increase not only the activity but also the stability of Pd catalysts. For example, Pires et al. [12] have synthesized PdM (M = Ni, Fe, Co) NPs with more stability compared with commercial Pd/C. Kim et al. [13] have prepared Pt NPs supported on carbon and modified it by irreversible adsorption of Bi(III) on Pt surfaces in which the Bi exists mainly in the form of Bi oxide.

In previous literatures, graphene oxide (GO) is firstly reduced to obtain the reduced GO (rGO) and then the rGO is used as support to prepare Pd/rGO [10], or the ions of Bi(III) are adsorbed on the surface of Pt particles [13] to obtain Bi(III) modified Pt/C. In this work, Bi has been introduced into Pd catalysts supported on the rGO by one-pot reaction in glycol under the irradiation of microwave (PdBi/rGO) to obtain the PdBi catalyst and the Bi exists mainly in Bi(0) form. The contents of Bi in the catalyst have influence on the electrooxidation of formic acid, and the optimum catalyst of PdBi/rGO exhibits the better performance compared with Pd/rGO and commercial Pd/C.

2. Experimental

2.1. Reagents and chemicals

Nafion solution (5 wt.%) was obtained from Aldrich and the Pd/C (30 wt.%) was bought from Johnson Matthey Corp. $PdCl_2$ and $Bi(NO_3)_3 \cdot 5H_2O$ were purchased from Sinopharm Chemical Reagent Co., Ltd. (Shanghai, China). All other reagents were of analytical grade and used without further purification.

2.2. Synthesis of catalysts

GO was synthesized according to literature [14] and the catalysts were prepared by a one-pot microwave reduction method. Briefly, 0.58 mL $PdCl_2$ (50 mM) and different quantities of $Bi(NO_3)_3 \cdot 5H_2O$ were dissolved in 2.18 mL of GO suspension (5 mg mL^{-1}) to form the mixtures with Bi:Pd atomic ratios of 0, 1:30, 1:20 and 1:10. The mixture

* Corresponding authors. Tel.: +86 351 7010699.
E-mail address: han_gaoyis@sxu.edu.cn (G. Han).

1566-7367/$ – see front matter © 2013 Elsevier B.V. All rights reserved.
http://dx.doi.org/10.1016/j.catcom.2013.12.014

was then dropped into 50 mL glycol under vigorous stir and then adjusted the pH to about 13 with 2 M KOH solution. The mixture was then heated under microwave irradiation (600 W) to 160 °C and kept for 5 min. Finally, the obtained solid was filtered, washed with water and dried at 70 °C under vacuum for 2 h. The resultant samples were defined as Pd/rGO, $PdBi_{0.03}$/rGO, $PdBi_{0.05}$/rGO and $PdBi_{0.10}$/rGO. The obtained catalysts of Pd/rGO and PdBi/rGO had a theoretical Pd loading of 30 wt.%.

2.3. Characterization and measurements

The morphologies of samples were characterized using a transmission electron microscopy (TEM, JEOL-2010) operating at 200 kV. X-ray diffraction (XRD) patterns were recorded on Bruker D8 Advance X-ray diffractometer with Cu *K*a radiation. X-ray photoelectron spectroscopies (XPS) were performed on Axis Ultra DLD (Kratos Shimadzu) spectrometer operating at 150 W. Electrochemical measurements were carried out on a CHI660B electrochemistry workstation by using a conventional three-electrode technique. The pre-polished pyrolytic graphite electrode (0.09 cm^2) loaded with catalysts (in terms of Pd: 33.3 μg cm^{-2}) was used as the working electrode while Pt plate and saturated calomel electrode (SCE) were used as counter and reference electrode, respectively. The electrolyte was 0.5 M H_2SO_4 solution with or without HCOOH. High-purity N_2 was bubbled into the solution for 10 min to remove O_2 and maintained during the electrochemical measurements. All the electrochemical measurements were performed at a temperature of 25 ± 1 °C.

3. Results and discussion

As observed from Fig. 1A, the rGO shows the typical sheet structure with crimples. The commercial Pd/C catalyst shows that the Pd particles with an average size of about 5.2 nm disperse on the carbon support (Fig. 1B). It is found that the Pd particles dispersed on rGO are relatively uniform and their average size is about 4.7 nm (Fig. 1C), indicating that the rGO may cause the Pd particles size small. The particles in both samples of $PdBi_{0.03}$/rGO (Fig. 1D) and $PdBi_{0.05}$/rGO (Fig. 1E) also exhibit a relatively uniform distribution and the size of the particles ranges from 2 to 9 nm, which is similar to that of Pd/rGO. However, particles in $PdBi_{0.10}$/rGO are not uniform and have some aggregation, the scale of the particles ranges from 3 to 11 nm (Fig. 1F). The result demonstrates that the addition of little Bi has almost no influence on the size of particles and that more content of Bi can make the size increase and aggregation of particles.

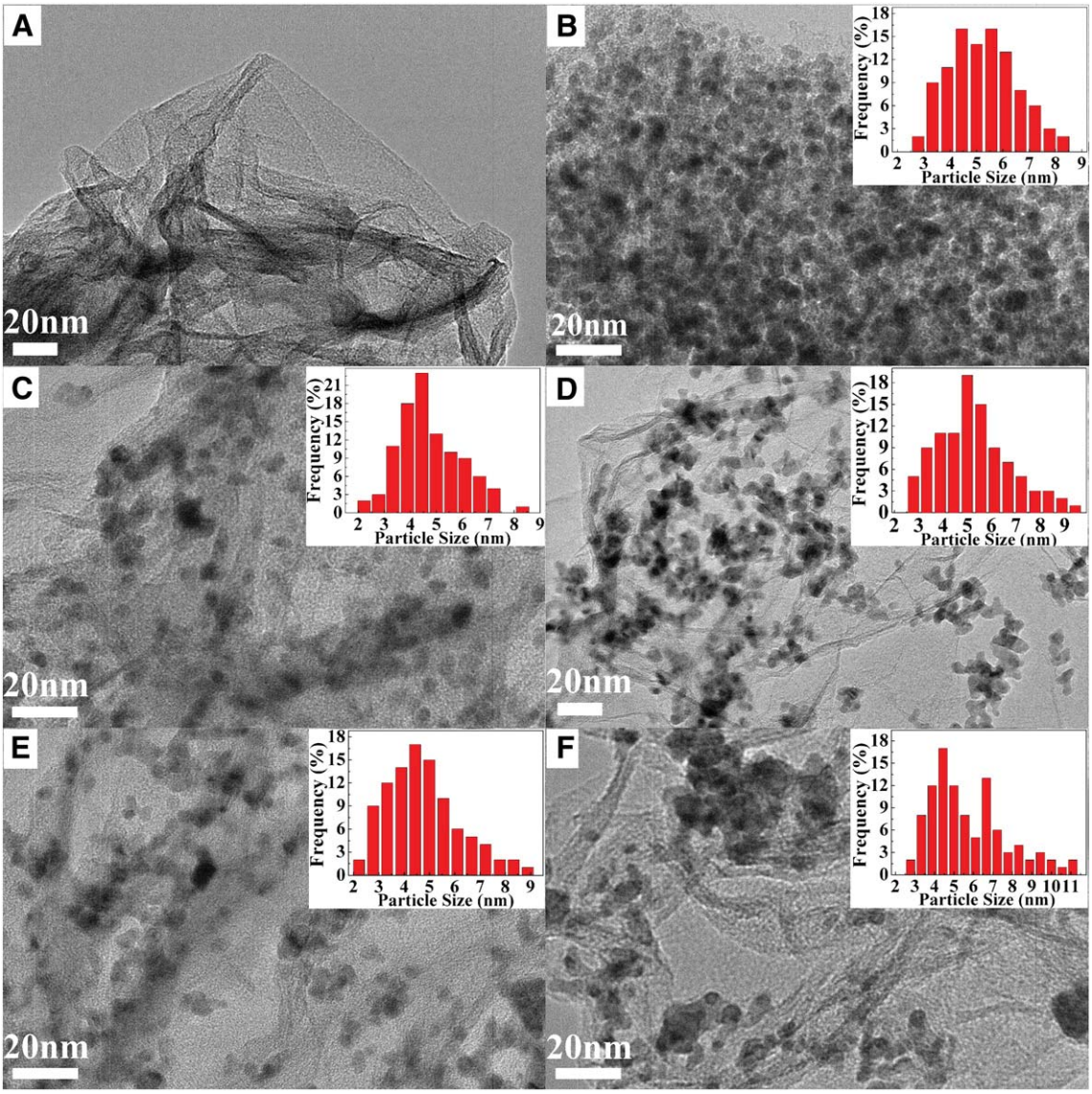

Fig. 1. The TEM images of rGO (A), commercial Pd/C (A), Pd/rGO (C), $PdBi_{0.03}$/rGO (D), $PdBi_{0.05}$/rGO (E) and $PdBi_{0.10}$/rGO (F).

The diffraction peaks (Fig. 2A) observed at about 25° in all samples may refer to C(002) plane of the supports while the peaks at about 40, 47 and 68° are corresponding to the diffraction of Pd(111), (200) and (220) plane, respectively [2,4]. For PdBi/rGO catalysts, the diffraction peaks of the Pd (fcc) phase are shifted to small angles compared with Pd/rGO and Pd/C catalysts, indicating that there is a lattice expansion because the relatively large Bi atoms have incorporated into Pd lattice [15]. Besides the Pd phase and the C(002) contribution, the strong broad peak ranged from 15 to 37° has also been observed in $PdBi_{0.10}$/rGO, which can be attributed to the presence of Bi and/or Bi_2Pd phases [16]. No obvious diffraction peaks related to Bi or Bi_2Pd phases are found in $PdBi_{0.03}$/rGO and $PdBi_{0.05}$/rGO because the Bi content is low or these species may exist in amorphous phases. The average sizes of the particles are calculated to be about 5.2, 4.4, 4.5, 4.3 and 5.2 nm for Pd/C, Pd/rGO, $PdBi_{0.03}$/rGO, $PdBi_{0.05}$/rGO and $PdBi_{0.10}$/rGO based on the Debye–Scherrer formula, which is almost consistent with the results of TEM images.

As observed from the XPS spectra shown in Fig. 2B, the GO shows C1s peaks at 284.5 and 286.8 eV, which can be ascribed to sp^2 hybridized carbon and the carbon related to the C–O bonds (Fig. 2B-a), respectively. Similar to the Pd/C catalysts (Fig. 2B-b), the samples of PdBi/rGO (Fig. 2B-c–f) possess strong sp^2 hybridized carbon peak at 284.6 eV, but weak peak related to the C–O bonds compared with GO, which indicates that GO has been reduced during the process of synthesis because glycol can act as a reducing agent under alkaline condition. The Pd3d XPS peaks (Fig. 2C) consist of three doublets which can be assigned to metallic Pd(0), PdO_{ads} and PdO species, respectively [17,18]. It is interesting to find that commercial Pd/C contains more PdO species than Pd(0), and that $PdBi_{0.05}$/rGO contains more Pd(0) species than other samples. The Bi4f XPS peaks can be fitted by three peaks which correspond to Bi(0), Bi(III) and BiO_{ads} species (Fig. 2D), and it is found that the presence of Bi in the particles is favorable to the Pd(0) species compared with literature [13]. The atomic ratio of Bi/Pd in PdBi/rGO determined by XPS is close to the molar ratio of the respective precursors utilized in the synthesis.

Fig. 3A shows that the sample of $PdBi_{0.05}$/rGO exhibits the relatively higher catalytic activity toward formic acid oxidation than other samples. Therefore $PdBi_{0.05}$/rGO is chosen to compare with commercial Pd/C and Pd/rGO. According to Fig. 3B, the electrochemical surface area (ECSA) can be calculated based on the integrated area of the reduction peak of Pd oxide at about 0.45 V [7,19], and the values of ECSA are calculated to be about 18.6, 24.5 and 23.3 $m^2\ g^{-1}$ for the commercial Pd/C, Pd/rGO and $PdBi_{0.05}$/rGO, respectively. This result reveals that Pd/rGO and $PdBi_{0.05}$/rGO have more Pd active sites than Pd/C. Moreover, it is also found that the reduction peak of Pd oxide in $PdBi_{0.05}$/rGO shifts to positive potential compared with Pd/C and Pd/rGO, indicating that Pd oxide is easily reduced in $PdBi_{0.05}$/rGO.

The electrocatalytic activities of the catalysts for formic acid oxidation have been evaluated by using CV in 0.5 M H_2SO_4 + 0.5 M HCOOH at a scan rate of 50 mV s^{-1}. As shown in Fig. 3C, the $PdBi_{0.05}$/rGO exhibits the best activity for formic acid oxidation with a peak current density of 1340 mA mg^{-1}, which is 1.5 times as large as that on Pd/rGO (890 mA mg^{-1}) and 2.7 times as large as that on commercial Pd/C catalysts (490 mA mg^{-1}). This result is better than PdNi/C reported previously [2], and indicates that the addition of small amount of Bi can greatly enhance the kinetics for formic acid oxidation. This may be that Bi can increase efficiency of Pd active sites because the addition of Bi may weaken the accumulation of CO-like intermediates although the

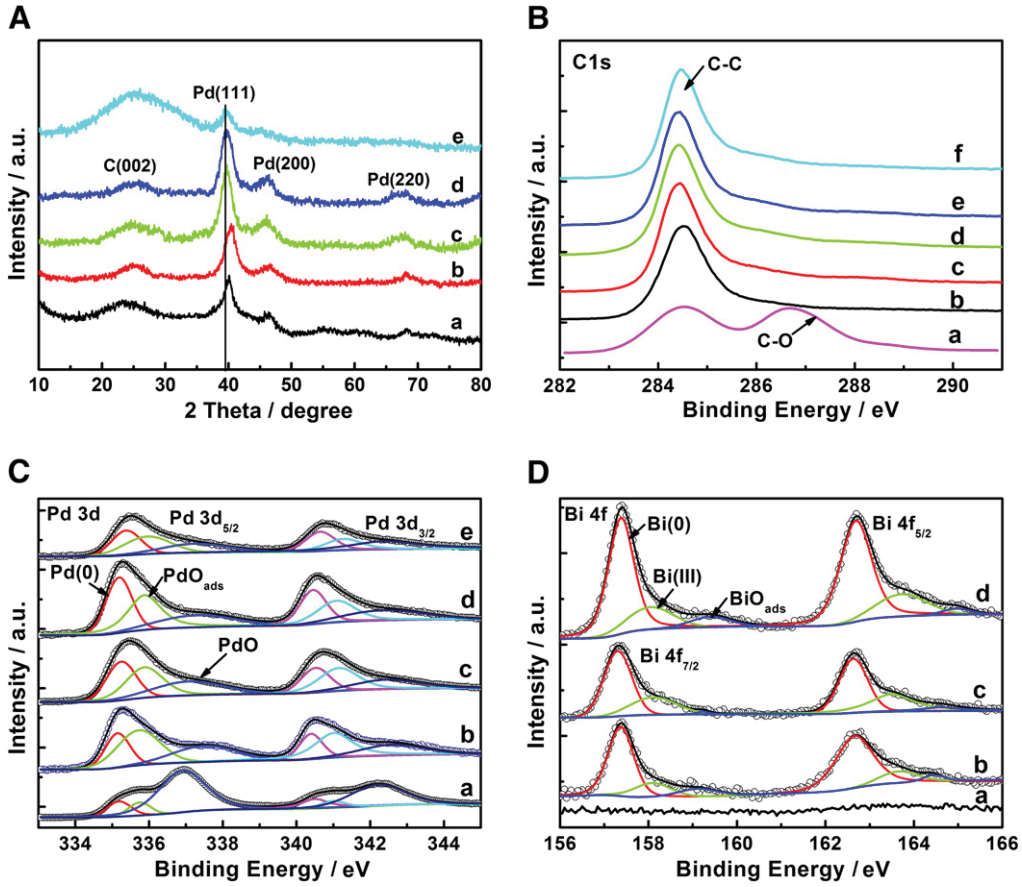

Fig. 2. (A) The XRD patterns of commercial Pd/C (a), Pd/rGO (b), $PdBi_{0.03}$/rGO (c), $PdBi_{0.05}$/rGO (d) and $PdBi_{0.10}$/rGO (e), (B) The C1s XPS spectra of GO (a), Pd/C (b), Pd/rGO (c), $PdBi_{0.03}$/rGO (d), $PdBi_{0.05}$/rGO (e) and $PdBi_{0.10}$/rGO (f), (C) Pd3d XPS spectra in the catalysts of Pd/C (a), Pd/rGO (b), $PdBi_{0.03}$/rGO (c), $PdBi_{0.05}$/rGO (d) and $PdBi_{0.10}$/rGO (e) and (D) Bi 4f XPS spectra of Pd/rGO (a), $PdBi_{0.03}$/rGO (b), $PdBi_{0.05}$/rGO (c) and $PdBi_{0.10}$/rGO (d).

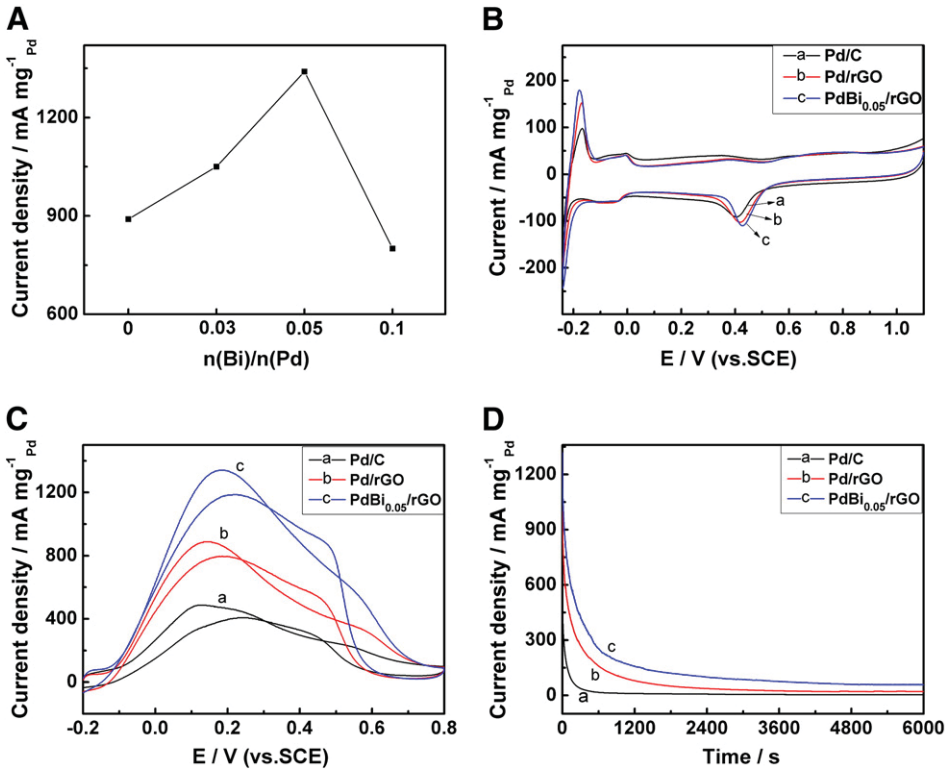

Fig. 3. The plot of the peak current density for the formic acid oxidation on the catalysts with different Bi/Pd ratios (A), the cyclic voltammograms of the catalyst in 0.5 M H_2SO_4 (B) and in 0.5 M H_2SO_4 + 0.5 M HCOOH at a scan rate of 50 mV s^{-1} (C) and the chronoamperometry curves of catalysts in 0.5 M H_2SO_4 + 0.5 M HCOOH at 0.2 V (D). (a) Pd/C, (b) Pd/rGO and (c) $PdBi_{0.05}$/rGO.

addition of a small amount of Bi may take up some Pd active sites compared with Pd/rGO based on the ECSA result.

From the chronoamperometric curves (Fig. 3D), it can be observed that the current density for formic acid oxidation on the $PdBi_{0.05}$/rGO after 6000 s is higher than that on commercial Pd/C and Pd/rGO at the corresponding time. This illustrates that the stability of $PdBi_{0.05}$/rGO catalysts is better than that of the commercial Pd/C and Pd/rGO. It may be that crystal lattice of Pd has changed and enhanced the OH_{ads} adsorbed on Pd sites adjacent to Bi, which facilitates the oxidative removal of CO-like intermediates by the OH_{ads} species and improves the kinetics for formic acid oxidation when optimum Bi atom dope into Pd lattice [20].

4. Conclusions

PdBi particles dispersed on rGO have been synthesized through one-pot reaction under microwave irradiation. The PdBi alloy phase increases in PdBi/rGO with the increment of Bi content in the composites. The resultant $PdBi_{0.05}$/rGO shows high activity and good stability toward the electrooxidation of formic acid, which reveals that optimum quantities of Bi may decrease the agglomeration of Pd particles or increase the toleration to CO-like intermediates. This approach can be extended to prepare other noble metals or their alloyed NPs supported on rGO.

Acknowledgments

Thanks to NSF of China (21274082 and 21073115) and Shanxi province (2012021021-3), the Program for NCET in University (NCET-10-0926) and Research Project supported by Shanxi Scholarship Council of China (2011-003).

References

[1] X. Yu, P.G. Pickup, J. Power Sources 182 (2008) 124–132.
[2] L. Shen, H. Li, L. Lu, Y. Luo, Y. Tang, Y. Chen, T. Lu, Electrochim. Acta 89 (2013) 497–502.
[3] Y. Zhu, S. Ha, R.I. Masel, J. Power Sources 130 (2004) 8–14.
[4] Y. Lee, S. Han, A. Ko, H. Kim, K. Park, Catal. Commun. 15 (2011) 137–140.
[5] X. Yu, P.G. Pickup, Electrochem. Commun. 11 (2009) 2012–2014.
[6] Y. Zhu, Z. Khan, R.I. Masel, J. Power Sources 139 (2005) 15–20.
[7] Y. Jiang, Y. Lu, F. Li, T. Wu, L. Niu, W. Chen, Electrochem. Commun. 19 (2012) 21–24.
[8] Z. Tian, S. Jiang, Y. Liang, P. Shen, J. Phys. Chem. B 110 (2006) 5343–5350.
[9] K.M. Metz, D. Goel, R.J. Hamers, J. Phys. Chem. C 111 (2007) 7260–7265.
[10] R.C. Cerritos, V. Baglio, A.S. Aricò, J.L. García, M.F. Sgroi, D. Pullini, A.J. Pruna, D.B. Mataix, R.F. Ramírez, L.G. Arriaga, Appl. Catal. B 144 (2014) 554–560.
[11] Z. Bai, L. Yang, J. Zhang, L. Li, J. Lv, C. Hu, J. Zhou, Catal. Commun. 11 (2010) 919–922.
[12] F.I. Pires, H.M. Villullas, Int. J. Hydrogen Energy 37 (2012) 17052–17059.
[13] B.J. Kim, K. Kwon, C.K. Rhee, J. Han, T.H. Lim, Electrochim. Acta 53 (2008) 7744–7750.
[14] Y. Chang, G. Han, M. Li, F. Gao, Carbon 49 (2011) 5158–5165.
[15] Z. Liu, X. Zhang, L. Hong, Electrochem. Commun. 11 (2009) 925–928.
[16] F. Dawood, B.M. Leonard, R.E. Schaak, Chem. Mater. 19 (2007) 4545–4550.
[17] I.G. Casella, M. Contursi, J. Electroanal. Chem. 588 (2006) 147–154.
[18] T. Ohmori, M.S. El-Deab, M. Osawa, J. Electroanal. Chem. 470 (1999) 46.
[19] E. Lim, H. Kim, W. Kim, Catal. Commun. 25 (2012) 74–77.
[20] M.M. Tusi, N.S.O. Polanco, S.G. daSilva, E.V. Spinace, A.O. Neto, Electrochem. Commun. 13 (2011) 143–146.